PPPL-2214

UC20-A,F

DR-1020-0 PPPL-2214

I- 21088

GLOBAL MAGNETIC FLUCTUATIONS IN S-1 SPHEROMAK PLASMAS AND RELAXATION TOWARD A MINIMUM-ENERGY STATE

By

A. Janos, G.W. Hart, C.H. Nam, and M. Yamada

MAY 1985

PLASMA PHYSICS LABORATORY

PRINCETON UNIVERSITY

PRINCETON, NEW JERSEY

PREPARED FOR THE U.S. DEPARTMENT OF ENERGY,
UNDER CONTRACT DE-AC02-76-CHO-3073.

GLOBAL MAGNETIC FLUCTUATIONS IN S-1 SPHEROMAK PLASMAS AND RELAXATION TOWARD A MINIMUM-ENERGY STATE

A. Janos, G.W. Hart, C.H. Nam, and M. Yamada

PPPL--2214

DE85 011365

ABSTRACT

Globally coherent modes have been observed during formation in the S-1 Spheromak plasma by analysis of magnetic field fluctuations measured from outside the plasma. The modes are of low n number ($2 \leq n \leq 5$), where n is defined by the functional dependence $e^{in\phi}$ of the fluctuation on toroidal angle ϕ. These modes are shown to be related to flux conversion and plasma relaxation toward a minimum-energy state during the spheromak formation. The modes are active while the q profile is rapidly changing, with q on-axis, q_o, rising to 0.7. A significant finding is the temporal progression through the n = 5, 4, 3, 2; m = 1 mode sequence as q rises through rational fractions m/n. During formation, peak amplitudes of the n = 2, 3, 4 modes relative to the unperturbed field have been observed as high as 20%, while more typical amplitudes are below 5%.

I. INTRODUCTION

Many schemes for the toroidal magnetic confinement of fusion plasmas involve configurations with both poloidal and toroidal fields. Poloidal and toroidal denote the short and long way, respectively, around the torus. The poloidal and toroidal fields of two closely related configurations, the reversed-field pinch[1] (RFP) and the spheromak,[2] are sustained mainly by toroidal and poloidal currents in the plasma. Spheromaks are established without toroidal field coils linking the toroidal plasma, and the toroidal field is maintained entirely by plasmas currents. An interesting feature of these two configurations is magnetic flux conversion[3] between the poloidal and toroidal fields. This conversion is important for relaxation of these plasmas toward a stable, minimum-energy Taylor state.[4] Also, sustainment of these discharges is made possible by utilization of this relaxation phenomena.[5-7] The relaxation process is often accompanied by magnetic field fluctuations[1,5,8-14] which are thought to be one possible mechanism for the relaxation process. Relaxation in spheromaks was first evidenced by the plasma's maintenance of equilibrium profiles close to the lowest-energy, force-free eigenmodes predicted by theory.[15-17]

In recent S-1 Spheromak experiments,[18,19] flux conversion between the poloidal and toroidal fluxes of the plasma was observed during and after formation of the plasma. Plasmas were observed to adjust themselves during formation such that the ratio of the toroidal plasma current to toroidal magnetic flux in the plasma, I/Φ, was a constant independent of initial conditions such as capacitor bank voltages. The Taylor state is characterized by the force-free condition $\underline{j} = \lambda \underline{B}$ where λ is a constant independent of position, j is current density and B is magnetic field. If λ is constant, then λ also equals I/Φ by simple integration. Since λ experimentally is found

to deviate from a constant value, I/Φ can be taken to be an "average λ" value. I/Φ is proportional to the pinch parameter $\theta \equiv 2I/aB_o$ of RFP research through a simple geometric factor involving the plasma size. The time behavior of I/Φ in S-1 was very similar to that of θ in RFP discharges. It was experimentally observed in S-1 that this I/Φ ratio was maintained for the duration of a discharge. If the plasma evolved after formation such that the I/Φ ratio deviated too far from an acceptable range, then relaxation oscillations, with the associated precursor oscillations, restored I/Φ to a range commensurate with that theoretically predicted on the basis of a force-free, minimum-energy state equilibrium. The theoretical value of I/Φ, in MA/Vsec, based on a classical spherical-boundary spheromak configuration, is $3.581/r_c$, where r_c is the separatrix radius in meters. In an attempt to understand further these phenomena, a magnetic coil system external to the plasma was installed to 1) look for possible toroidal mode structure of the magnetic fluctuations, and 2) monitor the gross behavior of the spheromak plasma (shift/tilt). Long-lived (~ 0.5 ms) spheromak plasmas almost completely detached from the flux core were produced. Well-defined modes with an assumed form $e^{i(m\theta+n\phi)}$ are observed almost always during the formation phase, with n in the range 1 to 5, where θ is the poloidal angle and ϕ is the toroidal angle. These modes are important for two reasons: they can play an important function in the relaxation of these plasmas toward a minimum-energy state; and they probably negatively affect energy and particle confinement.

The important relation of these modes to flux conversion and relaxation during formation and to the evolution of the $q(\Psi)$-profile is demonstrated, where q is the usual "safety factor" of tokamak terminology and Ψ is the poloidal flux. A significant finding is the temporal progression of the MHD activity through an n = 5, 4, 3, 2; m = 1 mode sequence during formation.

This is shown to correspond with the time evolution of the central q through the rational fractions m/n = 1/5, 1/4, 1/3, 1/2 to a final value of ~ 0.7. This progression is analogous to that for magnetic oscillations seen in a tokamak during the start-up phase. Experimental and theoretical data suggest that these modes in S-1 are probably internal resistive MHD instabilities originating on rational surfaces in the plasma.

Section II contains a discussion of the experimental details and the manipulation of the data. Section III describes the behavior of the modes and their relation to plasma relaxation and the q profile. Section IV contains a summary and conclusions.

II. EXPERIMENTAL APPARATUS AND MAGNETIC PROBE DATA ACQUISITION AND ANALYSIS

The plasma formation in the S-1 type of spheromak device is based on an inductive transfer of toroidal and poloidal magnetic flux from a toroidal "flux core" to the plasma.[15] Figure 1 shows a cross section of the S-1 device displaying the vacuum vessel, equilibrium field coils, flux core, Figure-8 stabilization coil system,[20] n-mode diagnostic coil arrays, and plasma. The experimentally obtained contours of constant poloidal flux towards the end of the formation phase wherein the spheromak configuration is not completely detached from the flux core are also shown in Fig. 1.

The formation process proceeds as follows. Initially, a steady-state poloidal equilibrium field is generated to support the final plasma equilibrium. A poloidal field generated by a toroidal current inside the flux core is pulsed on (see Fig. 2, bottom). The superposition of these two fields creates a field weaker on the small-major-radius side of the core. A toroidal solenoid inside the core is then pulsed on at time t = 0, and a plasma discharge is initiated. The increasing toroidal flux in this solenoid

induces a poloidal current in a toroidally concentric plasma surrounding the core. The associated toroidal field distends the plasma, stretching it towards the device axis where the polcidal field is weakest. Simultaneously the toroidal current in the core is reduced to induce a toroidal current in the plasma. Magnetic reconnection of the poloidal field occurs and a plasma toroid, the desired spheromak configuration, is created.

The S-1 device has been creating a plasma with a major radius of about 55 cm and a minor radius of about 30 cm. Toroidal plasma currents up to 350 kA are obtained. Peak plasma electron densities for the discharges reported herein range from 2×10^{13} cm^{-3} to 1×10^{14} cm^{-3}; measured electron temperatures range from 20 - 60 eV.

Stability against rigid-body $n = 1$ modes, provided by a passive Figure-8 stabilization coil system,[20] has allowed the formation of spheromaks which are nearly completely detached from the core and are sufficiently stable and long-lived ($\sim$ 0.5 msec) to allow the observation of the evolution of $n \geq 2$ modes as the plasma forms and decays. The results in this paper cover operation after installation of the Figure-8 coils.

Our investigations of the MHD fluctuations have utilized a variety of diagnostics. The h-mode diagnostic coil array consists of 16 pairs of magnetic pick-up coils distributed toroidally, at equal angles over the full 360°, inside the vacuum vessel at a major radius of R_o = 50 cm and an axial position of z_o = 60 cm (Fig. 1). The coils are located just outside of the Figure-8 coil system and the Figure-8 coil system is, in turn, outside the separatrix of the spheromak magnetic configuration. Each pair of coils measures the time derivative of the magnetic field components in the major radius direction ($\dot{B}_R$) and the toroidal direction ($\dot{B}_\phi$). The coils were

designed to measure magnetic field fluctuation levels of 1G (~ 0.1%) in a typical frequency range of 5-10 kHz. Coils are comprised of 50 turns with diameters of 0.77 cm (B_R) and 0.60 cm (B_ϕ). The high frequency cutoff of this coil system is 80 kHz, and at 200 kHz the signals are attenuated by a factor of approximately 2.5. An example of the $\dot{B}_R(t)$ data from the 16-channel array is shown in Fig. 2.

Globally coherent fluctuations, or modes, are often evident from the plot of the 16 channels of $\dot{B}$ versus time. When one mode is predominant, its n number can be determined simply by counting the number of maxima in $\dot{B}$ appearing in the 16 channels at an instant of time as can been seen in Fig. 2.

The $\dot{B}$ data are digitally integrated to obtain the magnetic fields as a function of toroidal angle ϕ and time t. These fields are then resolved into toroidal n-modes by use of discrete Fourier transformation[21] as follows:

$$B(\phi_k, t) = \sum_{n=0}^{N-1} B_n(t)\, e^{in\phi_k} \tag{1}$$

and

$$B_n(t) = \frac{1}{N} \sum_{k=0}^{N-1} B(\phi_k, t)\, e^{-in\phi_k} \tag{2}$$

$$\equiv c_n e^{i\alpha_n}$$

where $\phi_k = 2\pi k/N$, N is the number of coils (= 16) and k labels each coil. Considering the relation $B_{N-n} = B_n^*$, the amplitude of mode n is

$$\left.\begin{matrix} 2c_n \\ c_0 \\ c_8 \end{matrix}\right\} \text{for } n = \begin{cases} 1, 2, \ldots, 7 \\ 0 \\ 8 \end{cases}$$

and this is plotted versus time.

The q-value is the reciprocal of the rotational transform, $\iota = 2\pi/q$, and is conveniently calculated from $q \equiv d\Phi/d\Psi$ where Φ and Ψ are toroidal and poloidal fluxes, respectively. The time evolution of the $q(\Psi)$ profiles is experimentally determined as follows. The magnetic configuration is measured as a function of space and time with a movable multicoil magnetic probe inserted into the plasma. The time evolution of a magnetic field profile in major radius, R, is obtained on a single shot for fixed z (distance along device axis) and ϕ. A two-dimensional cross section of the plasma in a chosen R-z plane is then obtained by scanning this probe in the z-direction on a shot-to-shot basis. This plot requires data from approximately 40 consecutive and reproducible discharges. This yields a (R,z,ϕ,t) data array with spatial mesh size of 7.5 to 15 cm. B_z and B_ϕ data are then interpolated to produce a finer mesh. The poloidal flux function $\Psi = \int_0^R B_z \, 2\pi R \, dR$ is then calculated to determine the contours of constant Ψ, and the toroidal flux Φ enclosed by a constant Ψ surface is calculated. Figure 1 shows an example of the contours of constant poloidal flux in the R-z plane. The $q(\Psi)$-profile is obtained from $q(\Psi) = \Delta\Phi/\Delta\Psi$, where $\Delta\Phi$ is the difference in toroidal flux between two nearby surfaces Ψ and $\Psi + \Delta\Psi$.

Other diagnostics used to observe fluctuations include an ultra-soft (> 10 eV) X-ray detection system[22] to measure emissivity profiles. An array comprised of 19 silicon surface-barrier detectors views perpendicular to the midplane with the individual detectors viewing along chords at different major radii distances from the device axis. Also, a triple Langmuir probe is used to measure, at the plasma edge, time-resolved electron density and temperature.

III. DISCUSSION

A. Properties of Measured Modes

Well-defined modes of low n-number ($1 \leq n \leq 5$) are typically observed during formation from both the B_R and B_ϕ coils, and the B_R and B_ϕ data agree with respect to modes and their evolution. Since the n-mode diagnostic coils are outside the magnetic separatrix of the spheromak configuration, the toroidal field signals cannot be due to poloidal plasma currents. Instead, these modes must be associated with some helical deformation which generates a toroidal component of B from the unperturbed axisymmetric poloidal field.

The larger amplitude modes are easily seen on the $\dot{B}$ data, and sometimes even on the integrated B data, as disturbances periodic in ϕ with an integer number of periods around the torus. An example of $\dot{B}_R$ data exhibiting a well-defined $n = 3$ mode is shown in Fig. 2. The $n = 3$ mode is evident between $t = 0.15$ and 0.25 msec and is seen to be propagating in the direction of increasing "toroidal location number." Time $t = 0$ indicates the initiation of the plasma discharge. The signal before $t = 0$ is due to the pulsed poloidal vacuum field.

Fourier analysis of these fluctuations shows that these are well-defined modes with activity levels peaking midway through the formation phase and sometimes lasting into the post-formation phase. An example of this for a different discharge from above is shown in Fig. 3. There is usually one dominant mode present at a time and it has an amplitude well above (up to 20 times) the "background" level. Typical mode amplitudes are 5-10 times the background level. The low level background amplitude shows no clear evolution through a discharge. The imperfect alignment of the Figure-8 coils causes currents to be generated in them not only from the rise of the vacuum poloidal field but also from the axisymmetric formation of the spheromak discharge.

This is the largest source of the background. For the discharge in Fig. 2, the peak amplitude of the n = 3 mode is 20 times the background level.

Figure 3 represents a typical experimental measurement of the time evolution of mode amplitudes. In this case, an n = 3 mode starts developing at ~ 0.1 msec into the discharge, reaches its half maximum at 0.18 msec, its peak at 0.24 msec, decays to half maximum at 0.38 msec, and disappears by 0.45 msec. An n = 2 mode undergoes similar evolution, peaking at 0.32 msec. In this case, the formation phase is completed by 0.4 msec, and the discharge terminates at approximately 0.75 msec.

The n = 0 component of the measured B_R fields, which is primarily comprised of the unperturbed axisymmetric poloidal field of the spheromak configuration, is on the order of 0.5 to 1.0 kG, comparable to the peak toroidal and poloidal fields measured with magnetic probes internal to the plasma. Peak amplitudes of the n = 2, 3, 4 modes relative to the unperturbed field have been observed as high as 20%. More typical amplitudes are below 5%. After formation, amplitudes are less than 1%. These amplitudes are similar to those observed in magnetized-coaxial-gun generated spheromaks after injection into flux conservers.[13,23]

The n = 1 mode is most often associated with a shift or tilt of the plasma and leads ultimately to the termination of the discharge for well-detached plasmas. The n = 2 mode often rotates; the n = 3 and 4 modes almost always rotate. The rotation is always in the electron diamagnetic drift direction, V_{D_e}, same as the direction of propagation of magnetic field fluctuations observed in tokamaks.[24] The modes in S-1 have been been observed to rotate at velocities ranging from 0.12 to 1.2 × 10^6 cm/sec, approximately an order of magnitude slower than the Alfvén velocity. Occasionally, two modes are present simultaneously and it is observed that these two modes can

have rotation velocities differing by as much as a factor of three. This implies mode rotation is not associated with a rigid-body rotation of the plasma. Also, the rotation velocity often slows with time, indicating a possible dependence of the rotation velocity on magnetic field, electron density, or electron temperature.

Mode structures often do not make much more than one full toroidal rotation before diminishing or changing into another mode structure. Therefore, the growth and decay times of a mode are often on the same time scale as a period of revolution (~ 0.1 msec), while being much shorter than the discharge time. Nevertheless, a dominant magnetic-field-fluctuation frequency is easily read from the raw data or the Fourier-analyzed data when a mode is present. Observed frequencies range from 2 kHz to 10 kHz and above.

It should be stressed that the above-described modes are prevalent during formation and shortly thereafter. The MHD activity in the post-formation phase does not show such large-amplitude global fluctuations with the n-mode diagnostic system. However, in addition to the above-described modes, there are fluctuations which are locally but not globally coherent in ϕ with frequencies of 100 to 200 kHz. Amplitudes of these high frequency fluctuations are also on the order of $\tilde{B}/B \lesssim 5\%$. These fluctuations seem to be correlated between up to five or six adjacent coils, and are therefore localized in toroidal angles of 100° or less. High frequency fluctuations have also been observed earlier[18,19] on the total toroidal plasma current and total magnetic flux in the plasma. Whereas the fluctuation levels on the total current and flux were high only during formation, the levels measured by these local pickup coils persist throughout the discharge. High frequency fluctuations are also observed in other local measurements such as electron density, measured with Langmuir probes, and in line-integrated measurements

such as ultra-soft X-ray. These spatially localized fluctuations may be "modes" of higher n number with $n \gtrsim 10$. These will be studied elsewhere.

B. Evolution of Modes During Formation

The mode numbers which occur and the mode amplitudes are very dependent on the programming of the formation process. For typical operating conditions, modes $n = 2$ and 3 occur most often.

A significant finding is the observation of a temporal progression through the $n = 5, 4, 3, 2$ mode sequence during formation. Sequences are almost always from high n to lower n. The n^{th} mode usually is decaying while the $(n - 1)^{th}$ mode is growing. Figure 3 shows a typical time progression through a $n = 3, 2, 1$ mode sequence. Figure 4 shows the time evolution of the n^{th} component of $B_R(\phi)$ from the Fourier analysis for $n = 1$ through 4. The well-defined mode structures are evident. Higher n-mode lobes are often observed to develop into lobes of the lower n-mode structures.

The relative weakness of the $n > 4$ modes may be in part attributable to their development earlier in the formation process and hence their further distance from the magnetic coils. Occasionally, however, a strong well-defined $n = 4$ or 5 mode does appear.

The plasma always survives the $n > 1$ modes. Only the $n = 1$ leads to termination for well-detached plasmas, if the plasma does not simply decay away before shifting and/or tilting.

C. Mode Evolution and q-Profiles

This temporal progression of modes is reminiscent of that for the magnetic oscillations observed[25] during the start-up phase of a tokamak plasma as early as the 1970's. In the tokamak case, a progression of $m = 6, 5, 4, 3,$

2; n = 1 modes is observed as $q(\Psi)$ decreases and q = m/n rational surfaces enter the plasma. These modes rotate in the electron diamagnetic drift direction and are now believed to be due to tearing modes.[26,27] For the spheromak case, comparison of the time evolution of the $q(\Psi)$ profile with that of the modes also shows a close relationship.

Figure 5 represents the time evolution of $q(\Psi)$ versus Ψ derived from flux plots such as the one shown in Fig. 1. These flux plots represent an average behavior over many shots and therefore the modes are not evident on them. The right-hand side of each $q(\Psi)$ curve represents the magnetic axis (peak Ψ). The left-hand sides are not continued to $\Psi = 0$ (major axis of the spheromak) due to increasing experimental uncertainty in the computation of q as magnetic surfaces begin to extend beyond the measured range. The q-value at the magnetic axis, q_o, is observed to rise through the rational fractions 1/5, 1/4, 1/3, 1/2 midway through the formation phase. The temporal evolution of the modes described earlier follows a sequence of n = 5, 4, 3, 2; m = 1 during the precise time interval q_o is rising through q_o = m/n values, where n = 5, 4, 3, 2; m = 1. Once q_o > m/n, the m/n rational surface is inside the plasma.

It is interesting to compare the experimental observations to expectations from resistive stability analysis[28-30] of various spheromak equilibria. The experimentally observed temporal sequence of unstable modes agrees with the analysis of J. DeLucia et al.[28] Figure 6 shows the linear growth rate contours in the continuous space formed by nq_o and na/R from their work, where a and R are the minor and major radii of the spheromak. This figure corresponds to m = 1 perturbations. A straight line from the origin represents one possible equilibrium. The two lines labeled t_1 and t_2 represent two experimental equilibria during the magnetically active period of

spheromak formation, with $t_2 > t_1$. It is seen that for the t_1 curve, the n = 3 mode is resistive MHD unstable while the n = 2 mode is stable. Modes are more unstable the higher n is. For the t_2 curve, the n = 2 mode also becomes resistive MHD unstable. Theory also predicts[30] that higher n-modes (n > 4) nonlinearly saturate at low amplitudes. This may account for the experimental observation that n > 4 modes usually have low amplitudes compared to n = 2 and 3 modes. It is of additional interest that the experimental equilibria are never far from the least unstable configuration with $q_o R/a \sim 0.67$. It thus appears that these modes are due to internal resistive MHD instabilities.

There is good evidence that the poloidal mode structure of these fluctuations is m = 1. A dominant m = 1 mode structure is observed with the ultra-soft X-ray system during the time period of strong magnetic mode activity. Second, theoretical analysis[28] indicates that the m = 1 modes are most unstable.

Looking at $q(\Psi)$ in more detail, $q(\Psi)$ is zero at the start of the discharge due to the purely poloidal field configuration in vacuum. During the early part of the formation before closed flux surfaces develop (t < 0.24 msec), q rises away from the magnetic axis. Magnetic reconnection occurs after 0.24 msec allowing the formation of closed flux surfaces. Also the basic shape of the $q(\Psi)$-profile changes from one with a minimum at the magnetic axis before reconnection to one which is an increasing function of Ψ after reconnection starts. After formation (t > 0.4 msec), $q(\Psi)$ is a monotonically increasing function of Ψ from the separatrix (R ≈ ±80 cm) to q_o = 0.73 at the magnetic axis (R ≈ ±60 cm). This general profile is then maintained for the remainder of the discharge. For comparison, the classical spherical-boundary spheromak configuration[2] has $q_o \approx 0.82$, with q

monotonically decreasing to $q_s = 0.72$ on the separatrix; a classical spheromak with the same degree of oblateness as the experimental configuration has a q_o of 0.65, with q decreasing to 0.47 at the separatrix. The time evolution of modes is not shown for the discharges used in the calculation of $q(\Psi)$; however, there is sharp peaking of mode activity between 0.15 and 0.25 msec, with strong n = 3 and n = 2 components present. Both modes are often simultaneously at or above their half-maximum amplitude at some instant during the formation phase, leading to possible mode interaction. These modes and the effects of possible interaction between these modes, together with reconnection, probably help to change the shape of the $q(\Psi)$-profile.

It should be noted that early in the discharge ($t < 0.24$ msec) there are no closed flux surfaces which are detached from the core (that is, which do not encircle the flux core). The q function is numerically calculated nevertheless using data for which $|R| \leq 80$ cm. The error due to the toroidal flux not accounted for around the core is expected to be small for not too small Ψ. The calculated q is always a lower limit for the method used. A rough estimate of a typical deviation of the true q from that calculated is $+ 0.1$ at small Ψ ($\Psi \approx 0.02$ Vsec) for $t \approx 0.3$ msec. As closed flux surfaces develop, the portion of the $q(\Psi)$ curve corresponding to closed surfaces is indicated by bold lines.

D. Plasma Relaxation

It has been earlier reported[18,19] that flux conversion is a strong mechanism during spheromak formation in the S-1 Spheromak. There are several indications that these modes described above play a crucial role in the relaxation of the spheromak toward a minimum-energy state.[4]

Both these modes and the relaxation are most prevalent during formation. In some cases, the applied coil currents would be expected to produce an equilibrium far from the Taylor state if the fluxes were transferred directly into the plasma. However, there is observed to be a conversion of poloidal flux into toroidal flux or vice versa during formation. The plasma adjusts itself during formation to achieve a constant ratio between the poloidal and toroidal fluxes ($I/\Phi \propto \lambda$ = constant), independent of initial conditions. The data show a final equilibrium near the Taylor force-free, minimum-energy state. The q-profile evolution described above also suggests a relaxation.

A time evolution of the inventory of poloidal and toroidal fluxes shows that there is a sudden (relative to the formation time) and large exchange of fluxes during the period of strong mode activity midway through the formation; thereafter, a quiescent equilibrium is achieved. For the example to be described below, the poloidal flux captured by the spheromak is seen to drop precipitously during the same period that there is a sudden and large increase in the toroidal flux in the plasma. Figure 7 shows the time evolution of the poloidal and toroidal fluxes measured from the two-dimensional flux plots described above. Figure 7a shows the maximum poloidal flux Ψ_{max} defined by the integral $\int 2\pi R\, B_z dR$ from R=0 to $R=R_{max}$ where R is major radius and R_{max} is R at the magnetic axis if there is one, otherwise R_{max} is the inside major radius of the flux core. Each of the curves in Fig. 7b is the measured toroidal flux within a closed poloidal flux surface defined by a constant poloidal flux distance $|\Psi - \Psi_{max}|$ from Ψ_{max}. The $|\Psi - \Psi_{max}| = 0.06$ Vsec curve includes over 50% of the total toroidal flux. Comparison of Φ curves for different $|\Psi-\Psi_{max}|$ reveals that toroidal flux is increased throughout the plasma and especially deep within the configuration (small $|\Psi-\Psi_{max}|$). It

would be interesting to compare these results with a theoretical determination of the profile of the redistributed flux as a consequence of different instabilities, but this information apparently does not exist yet. As was stated above, there is a sharp peaking of n = 3 and 2 mode activity between t = 0.15 and 0.25 msec. It is precisely during this ~ 0.1 msec time period that the fluxes undergo dramatic changes. The peak poloidal flux drops by approximately 35% (~ 0.06 Vsec) as the toroidal flux increases by more than a factor of 6 (~ 0.025 Vsec). This behavior is interpreted as relaxation to a lower energy state. The formation phase in these discharges is completed by 0.4 msec.

After formation is complete, the poloidal flux is observed to decay slowly due to resistive losses. The toroidal flux is also observed to decay, but at a slower rate. This difference in decay rates may be due to a continuous low level of flux conversion during the decay phase.

IV. SUMMARY AND CONCLUSIONS

We have shown strong evidence that low n-number modes play an essential role in relaxation of the S-1 Spheromak plasma toward the Taylor state during formation, wherein there can be a large transfer of magnetic flux. The temporal evolution of modes through the n = 5, 4, 3, 2; m = 1 sequence parallels the rise of the experimentally measured q_o through m/n rational fractions. This is analogous to the evolution of magnetic oscillations observed during the start-up phase of a tokamak plasma in which a progression of m = 6, 5, 4, 3, 2; n = 1 modes is observed as q decreases and q = m/n rational surfaces enter the plasma. Experimental observations and comparison of theoretical predictions with experiment suggest that the modes observed in S-1 are probably resonant modes due to resistive MHD instabilities.

This progression due to the $q(\Psi)$-profile evolution distinguishes spheromaks formed by the S-1 induction technique from those formed by magnetized coaxial guns. In the latter case the $q(\Psi)$-profile begins with q high, after which q falls, so that a different progression of modes might be expected. In fact, such gun-generated spheromaks have been observed to display large n = 1 and 2 activity. Results from CTX[13] show that coherent rigidly rotating n = 1 and n = 2 modes are generated during the sustained and decaying phases of the discharge, respectively. According to ideal MHD,[31] these modes are nonresonant, but the n = 2 appears when q is just below 0.5.

The modes observed in S-1 are expected to affect energy confinement. In tokamaks, the energy confinement time decreases as mode amplitudes become large ($\simeq$ 1%). It is observed[27] in tokamaks that strong disruptions in the current rise phase can degrade the plasma quality throughout the remainder of the discharge; proper programming of the rate of current rise avoids these disruptions. A carefully programmed formation in spheromaks may minimize the bad effects of these modes. The effects of these modes in S-1 on plasma parameters have yet to be investigated in detail.

ACKNOWLEDGMENTS

The authors thank S. Jardin, for relating his extensive theoretical results to these experimental observations and R. Ellis, Jr. for his thorough review of this research and very useful discussion. This work was supported by the U.S. Department of Energy Contract No. DE-AC02-76-CHO-3073.

REFERENCES

[1]H.A.B. Bodin and A.A. Newton, Nucl. Fusion 20, 1255 (1980), and references therein.

[2]M.N. Bussac et al., in Proceedings of the Seventh International Conference on Plasma Physics and Controlled Nuclear Fusion Research, Innsbruck, Austria, 1978 (IAEA, Vienna, Austria, 1979), Vol. III, 249; H.P. Furth, J. Vac. Sci. Technol. 18, 1073 (1982).

[3]H. Alfvén, L. Lindberg, and P. Mitlid, J. Nucl. Energy, Part C: Plasma Physics, 1, 116 (1960); L. Lindberg and C. Jacobsen, Astrophys. J. 133, 1043 (1961).

[4]J.B. Taylor, in Proceedings of the Third Topical Conference on Pulsed High β Plasmas, UKAEA Culham Laboratory, U.K., 1975, p. 59; J.B. Taylor, Phys. Rev. Lett. 33, 1130-1141 (1974).

[5]C.A. Bunting, C.W. Gowers, K. Ogawa, D.C. Robinson, and M.R.C. Watts, in Proceedings of the Eighth European Conference on Controlled Fusion and Plasma Physics, Prague, Czech., 1977, p. 79.

[6]D.A. Baker et al., in Proceedings of the Ninth International Conference on Plasma Physics and Controlled Nuclear Fusion Research, Baltimore, Maryland, 1982 (IAEA, Vienna, Austria, 1983), Vol. I, 587, IAEA-CN-41/M-1.

[7]T.R. Jarboe et al., Phys. Rev. Lett. 51, 39 (1983).

[8]I.H. Hutchinson et al., Nucl. Fusion 24, 59 (1984).

[9]V. Antoni and S. Ortolani, Plasma Phys. 25, 799 (1983).

[10]T. Tamano et al., in Proceedings of the Ninth International Conference on Plasma Physics and Controlled Nuclear Fusion Research, Baltimore, Maryland, 1982 (IAEA, Vienna, Austria, 1983), Vol. I, 609, IAEA-CN-41/H-3.

[11]R.G. Watt and R.A. Nebel, Phys. Fluids 26, 1168 (1983).

[12]A.R. Sherwood, Bull. Am. Phys. Soc. 28, 1188 (1983).

[13]B.L. Wright, in Proceedings of the Sixth U.S. Symposium on Compact Toroid Research and the Fifth U.S.-Japan Joint Symposium on Compact Toroid Research, Princeton, N.J., 1984, pp. 5-8.

[14]R.S. Shaw et al., in Proceedings of Sixth U.S. Symposium on Compact Toroid Research and the Fifth U.S.-Japan Joint Symposium on Compact Toroid Research, Princeton, N.J., 1984, pp. 53-56.

[15]M. Yamada et al., Phys. Rev. Lett. 46, 188 (1981).

[16]J. Jarboe et al., Phys. Rev. Lett. 45, 1264 (1980).

[17]G. Goldenbaum et al., Phys. Rev. Lett. 44, 393 (1980).

[18]A. Janos, in Proceedings of the Sixth U.S. Symposium on Compact Toroid Research and the Fifth U.S.-Japan Joint Symposium on Compact Toroid Research, Princeton, N.J., 1984, pp. 97-102.

[19]M. Yamada et al., in Proceedings of the Tenth International Conference on Plasma Physics and Controlled Nuclear Fusion Research, London, UK, 1984 (IAEA, Vienna, Austria), IAEA-CN-44/D-III-3.

[20]S.C. Jardin and U. Christensen, Nucl. Fusion 21, 1665 (1981).

[21]For example, The Fourier Transform and Its Applications, 2nd. ed. (McGraw-Hill, NY, 1978)

[22]S.F. Paul et al., in Proceedings of the Sixth U.S.-Japan Joint Symposium on Compact Toroid Research, Hiroshima, Japan, 1984.

[23]K. Watanabe et al., in Proceedings of the Sixth U.S. Symposium on Compact Toroid Research and the Fifth U.S.-Japan Joint Symposium on Compact Toroid Research, Princeton, N.J., 1984, pp. 29-32.

[24]J.C. Hosea, C. Bobeldijk, and D.J. Grove, in Proceedings of the Fourth International Conference on Plasma Physics and Controlled Nuclear Fusion Research, Madison, USA, 1971 (IAEA, Vienna, Austria, 1971), Vol. II, 425-440, IAEA-CN-28/F-7.

[25]S.V. Mirnov and I.B. Semenov, Madison IAEA Conf., Nucl. Fusion. Suppl., 189-192 (1971); Sov. J. At. En. 30, 22-29 (1971); Sov. Phys. JETP 33, 1134-1137 (1971).

[26]L.A. Artsimovich, Nucl. Fusion 12, 215 (1972).

[27]R.S. Granetz, I.H. Hutchinson, and D.O. Overskei, Nucl. Fusion 19, 1587-1595 (1979).

[28]J. DeLucia, S.C. Jardin, and A.H. Glasser, Phys. Fluids 27, 1470-1482 (1984).

[29]S.C. Jardin, Nucl. Fusion 22, 629 (1982).

[30]J. DeLucia and S.C. Jardin, Phys. Fluids 27, 1773 (1984); R.B. White, D.A. Monticello, M.N. Rosenbluth, and B.V. Waddel, Phys. Fluids 20, 800 (1977).

[31]G. Marklin, in Proceedings of the Sixth U.S. Symposium on Compact Toroid Research and the Fifth U.S.-Japan Joint Symposium on Compact Toroid Research, Princeton, N.J., 1984, pp. 88-91.

FIGURE CAPTIONS

FIG. 1. Cross section of S-1 device showing vacuum vessel, equilibrium field coils, flux core, passive Figure-8 coil stabilization system, and the n-mode diagnostic. The experimentally obtained poloidal flux contours of a spheromak configuration towards the end of the formation phase are also shown.

FIG. 2. Time evolution of $\dot{B}_R$ for 16 toroidal angles. An obvious n = 3 mode is evident at t ~ 0.2 msec, propagating toroidally. Plasma is initiated at t = 0 .

FIG. 3. Mode amplitude versus time for modes n = 1, 2, 3, 4. This discharge shows a clear sequential time evolution of the n-modes. During the rise of the vacuum poloidal field prior to t = 0, the B_R system picks up n > 0 components of B_R in addition to the expected large n = 0 component. These are due to currents induced in the Figure-8 coils because of a slight misalignment with respect to the flux core.

FIG. 4. Time evolution of the n^{th} component of B_R for 16 toroidal angles for n = 1 through 4. This is the same discharge as in Fig. 3.

FIG. 5. Plots of $q(\Psi)$ versus time.

FIG. 6 Growth rate contours in the continuous space formed by nq_o and na/R. Growth rates are proportional to the integer labels. Stable, ideal MHD unstable, and resistive MHD unstable regions are distinguished by dashed curves. An equilibrium is represented by a straight line starting at the origin. Typical experimental equilibria during the period of strong mode activity are indicated at times t_1 and t_2 with $t_2 > t_1$.

FIG. 7. Time evolution of (a) maximum poloidal flux Ψ_{max} and (b) toroidal flux Φ included in the poloidal flux contour a distance $|\Psi-\Psi_{max}|$ from Ψ_{max}. There is a precipitous drop in Ψ_{max} and a concurrent sudden and large increase in Φ during the period of strong magnetic mode activity.

#85X0018

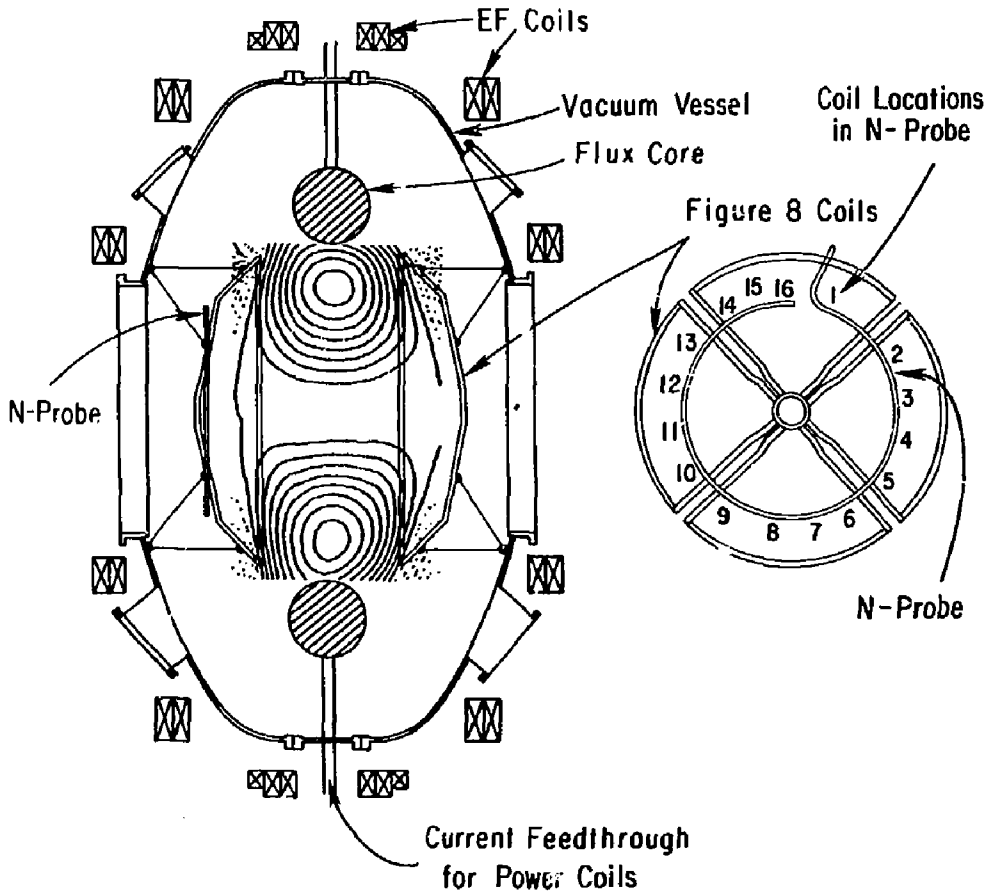

Fig. 1

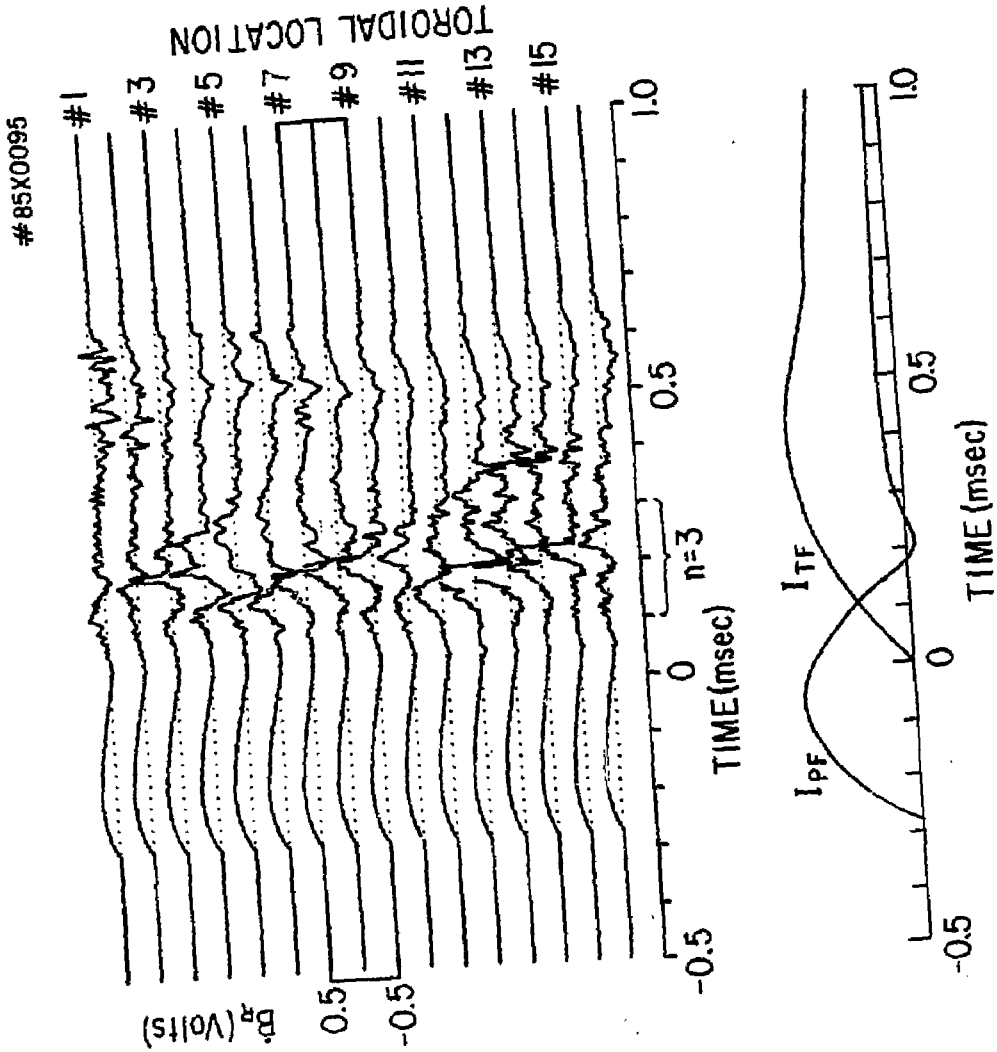
#85X0095
TOROIDAL LOCATION
#1
#3
#5
#7
#9
#11
#13
#15
$\dot{B}_R$ (Volts)
0.5
-0.5
1.0
0.5
0
-0.5
n=3
TIME(msec)
I_{TF}
I_{PF}
1.0
0.5
0
-0.5
TIME (msec)

Fig. 2

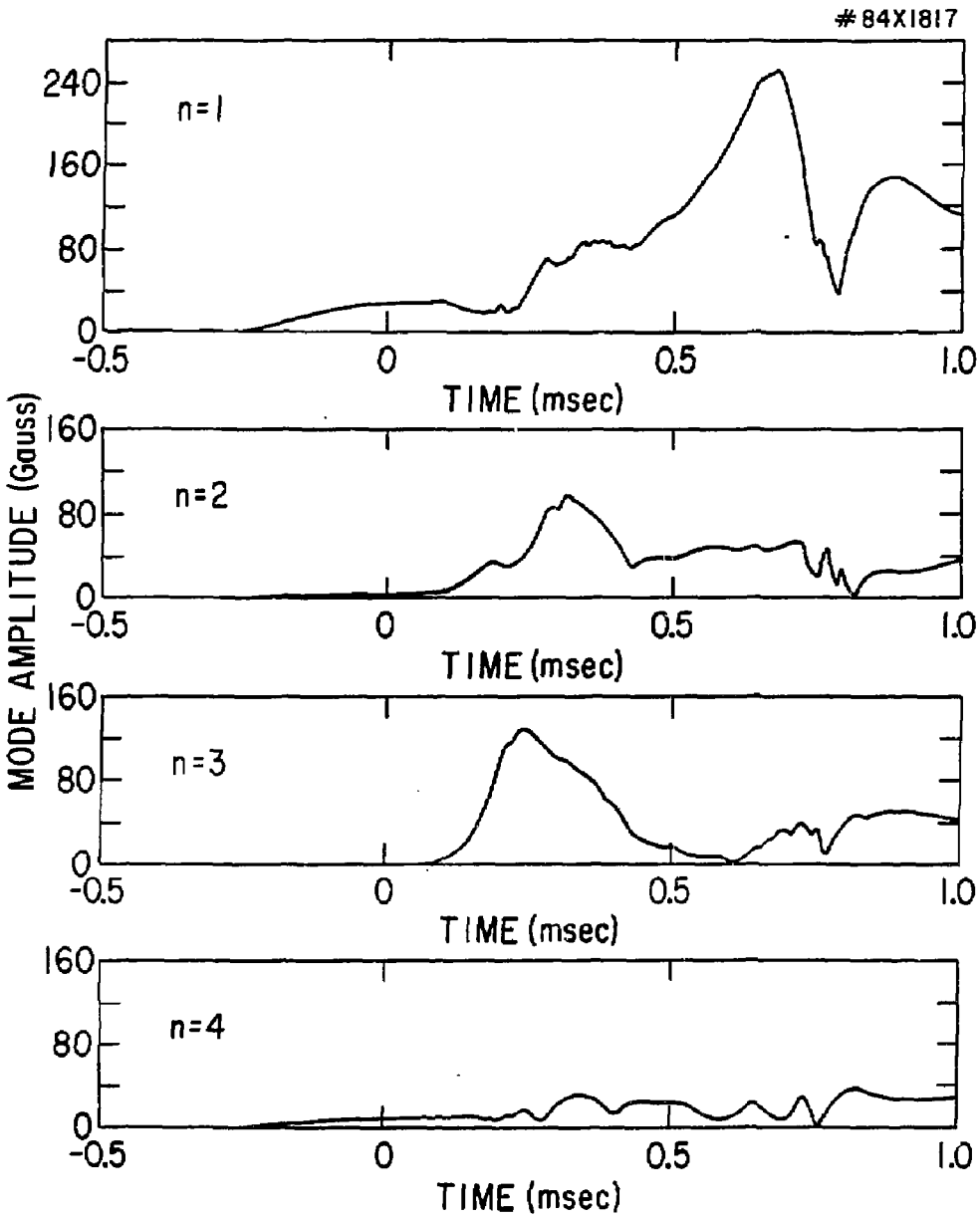
#84X1817
n=1
240
160
80
0
-0.5
0
0.5
1.0
TIME (msec)
MODE AMPLITUDE (Gauss)
n=2
160
80
0
n=3
n=4

Fig. 3

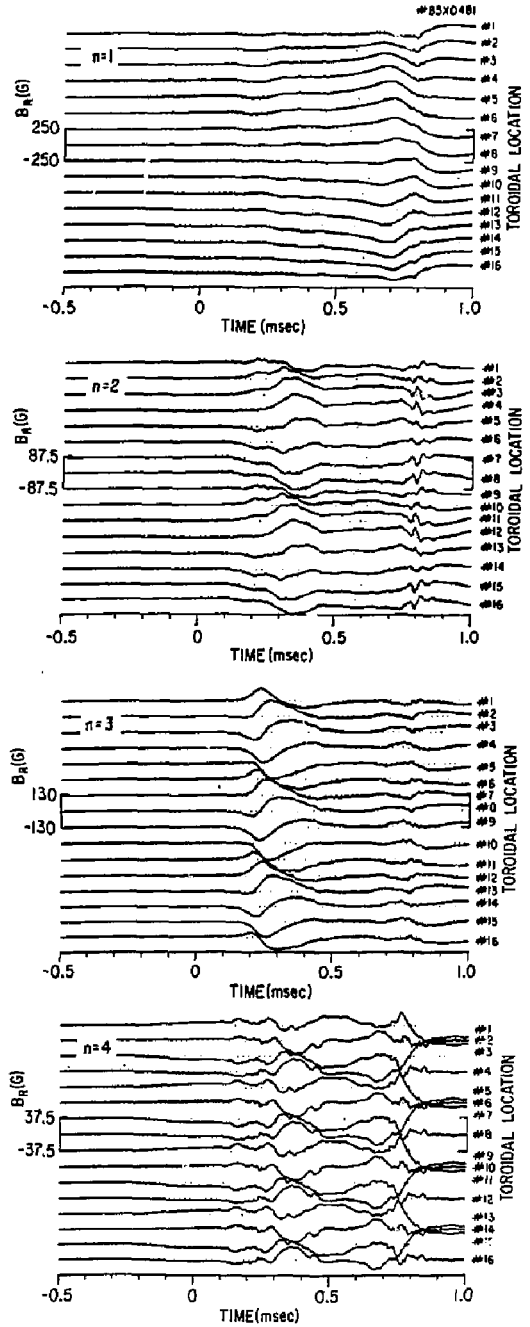
#85X0481
n=1
B_R(G)
250
-250
-0.5
0
0.5
1.0
TIME (msec)
TOROIDAL LOCATION
n=2
87.5
-87.5
n=3
130
-130
n=4
37.5
-37.5

Fig. 4

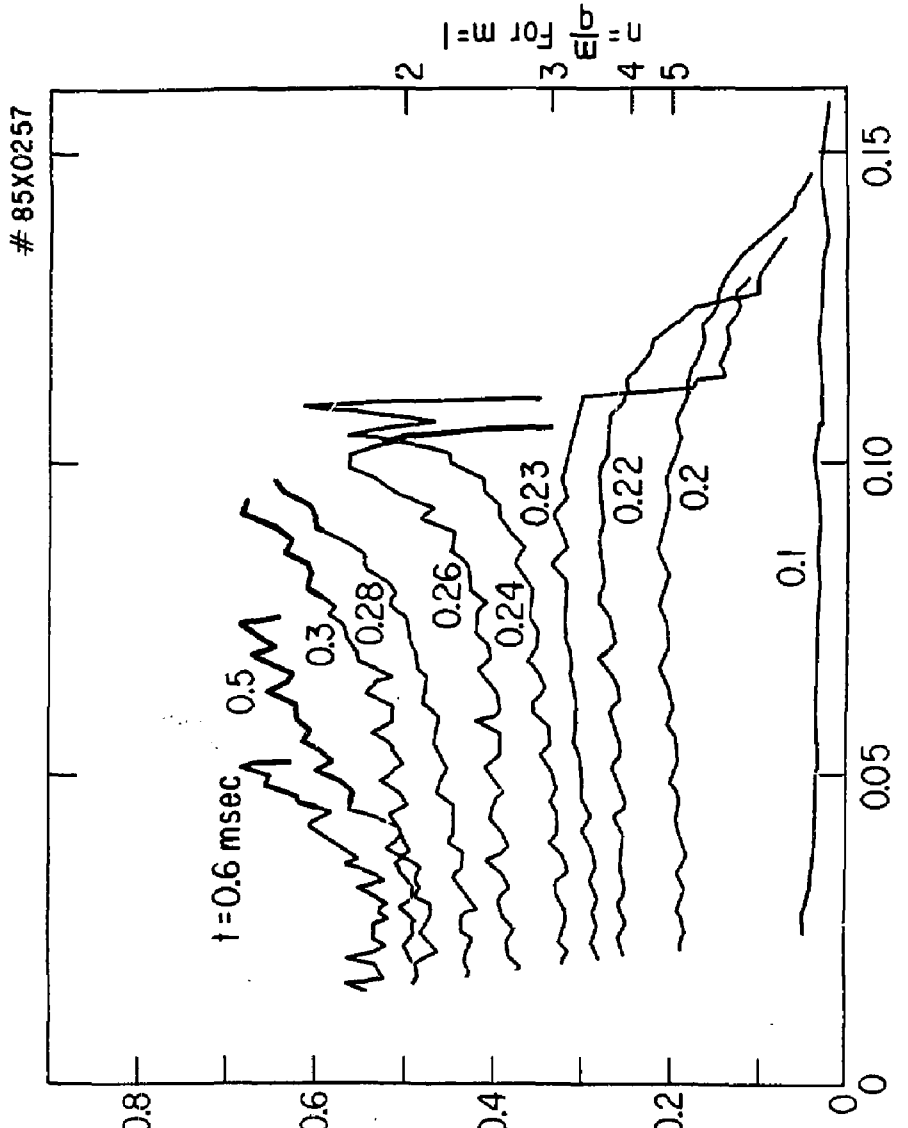
#85X0257
t=0.6 msec
0.5
0.3
0.28
0.26
0.24
0.23
0.22
0.2
0.1
q
ψ (V sec)
n = E/σ for m=1
0
0.05
0.10
0.15
0.2
0.4
0.6
0.8
2
3
4
5

Fig. 5

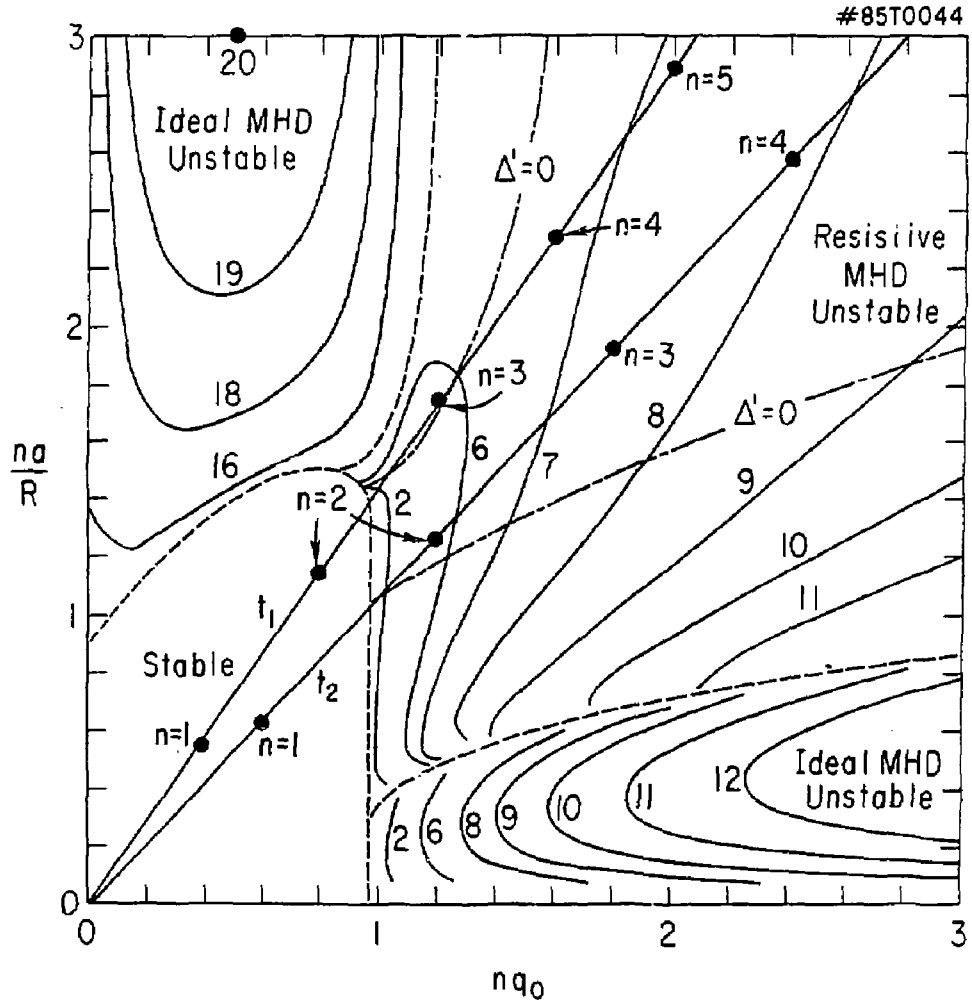
#85T0044
Ideal MHD
Unstable
Resistive
MHD
Unstable
Stable
Ideal MHD
Unstable
Δ'=0
Δ'=0
n=1
n=1
n=2
n=3
n=3
n=4
n=4
n=5
t1
t2
20
19
18
16
2
6
7
8
9
10
11
12
2
6
8
9
10
11
na/R
nq0
0
1
2
3

Fig. 6

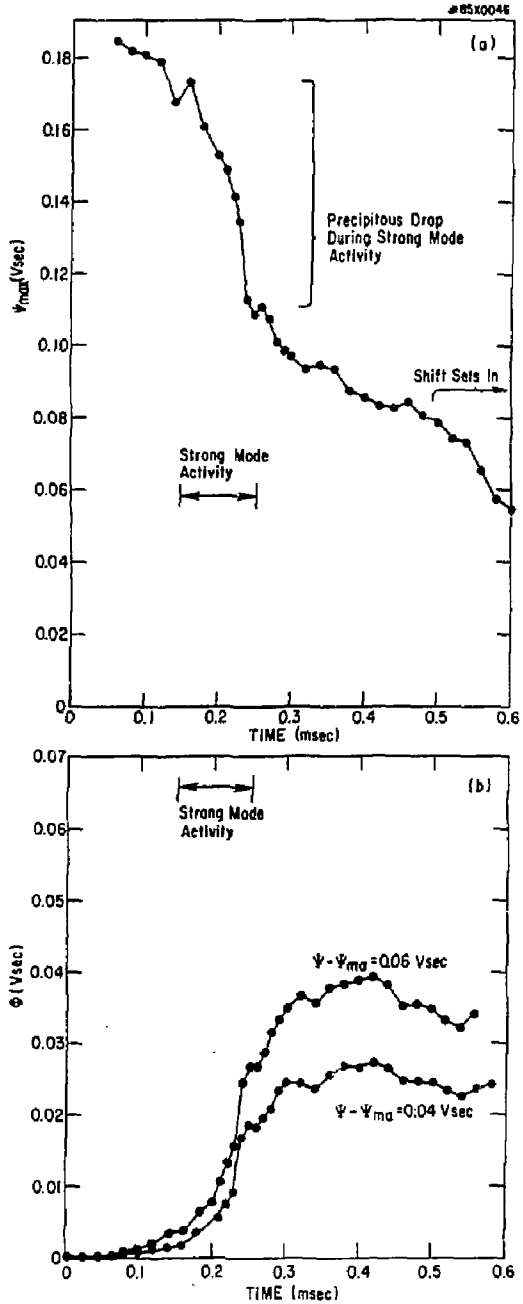
#85X0046
(a)
0.18
0.16
0.14
0.12
0.10
0.08
0.06
0.04
0.02
0
Ψ_{max}(Vsec)
Precipitous Drop
During Strong Mode
Activity
Shift Sets In
Strong Mode
Activity
0
0.1
0.2
0.3
0.4
0.5
0.6
TIME (msec)
(b)
Strong Mode
Activity
0.07
0.06
0.05
0.04
0.03
0.02
0.01
0
Φ (Vsec)
$\Psi - \Psi_{ma}$=0.06 Vsec
$\Psi - \Psi_{ma}$=0.04 Vsec
0
0.1
0.2
0.3
0.4
0.5
0.6
TIME (msec)

Fig. 7

EXTERNAL DISTRIBUTION IN ADDITION TO UC-20

Plasma Res Lab, Austra Nat'l Univ, AUSTRALIA
Dr. Frank J. Paoloni, Univ of Wollongong, AUSTRALIA
Prof. I.R. Jones, Flinders Univ., AUSTRALIA
Prof. M.H. Brennan, Univ Sydney, AUSTRALIA
Prof. F. Cap, Inst Theo Phys, AUSTRIA
Prof. Frank Verheest, Inst theoretische, BELGIUM
Dr. D. Palumbo, Dg XII Fusion Prog, BELGIUM
Ecole Royale Militaire, Lab de Phys Plasmas, BELGIUM
Dr. P.H. Sakanaka, Univ Estadual, BRAZIL
Dr. C.R. James, Univ of Alberta, CANADA
Prof. J. Teichmann, Univ of Montreal, CANADA
Dr. H.M. Skarsgard, Univ of Saskatchewan, CANADA
Prof. S.R. Sreenivasan, University of Calgary, CANADA
Prof. Tudor W. Johnston, INRS-Energie, CANADA
Dr. Hannes Barnard, Univ British Columbia, CANADA
Dr. M.P. Bachynski, MPB Technologies, Inc., CANADA
Chalk River, Nucl Lab, CANADA
Zhengwu Li, SW Inst Physics, CHINA
Library, Tsing Hua University, CHINA
Librarian, Institute of Physics, CHINA
Inst Plasma Phys, Academia Sinica, CHINA
Dr. Peter Lukac, Komenskeho Univ, CZECHOSLOVAKIA
The Librarian, Culham Laboratory, ENGLAND
Prof. Schatzman, Observatoire de Nice, FRANCE
J. Radet, CEN-BP6, FRANCE
AM Dupas Library, AM Dupas Library, FRANCE
Dr. Tom Mual, Academy Bibliographic, HONG KONG
Preprint Library, Cent Res Inst Phys, HUNGARY
Dr. S.K. Trehan, Panjab University, INDIA
Dr. Indra Mohan Lal Das, Banaras Hindu Univ, INDIA
Dr. L.K. Chavda, South Gujarat Univ, INDIA
Dr. R.K. Chhajlani, Vikram Univ. INDIA
Dr. S. Dasgupta, Saha Inst, INDIA
Dr. P. Kaw, Physical Research Lab, INDIA
Dr. Phillip Rosenau, Israel Inst Tech, ISRAEL
Prof. S. Cuperman, Tel Aviv University, ISRAEL
Prof. G. Rostagni, Univ Di Padova, ITALY
Librarian, Int'l Ctr Theo Phys, ITALY
Miss Clelia De Palo, Assoc EURATOM-ENEA, ITALY
Biblioteca, del CNR EURATOM, ITALY
Dr. H. Yamato, Toshiba Res & Dev, JAPAN
Direc. Dept. Lg. Tokamak Dev. JAERI, JAPAN
Prof. Nobuyuki Inoue, University of Tokyo, JAPAN
Research Info Center, Nagoya University, JAPAN
Prof. Kyoji Nishikawa, Univ of Hiroshima, JAPAN
Prof. Sigeru Mori, JAERI, JAPAN
Library, Kyoto University, JAPAN
Prof. Ichiro Kawakami, Nihon Univ, JAPAN
Prof. Satoshi Itoh, Kyushu University, JAPAN
Dr. D.I. Choi, Adv. Inst Sci & Tech, KOREA
Tech Info Division, KAERI, KOREA
Bibliotheek, Fom-Inst Voor Plasma, NETHERLANDS
Prof. B.S. Liley, University of Waikato, NEW ZEALAND
Prof. J.A.C. Cabral, Inst Superior Tecn, PORTUGAL
Dr. Octavian Petrus, ALI CUZA University, ROMANIA
Prof. M.A. Hellberg, University of Natal, SO AFRICA
Dr. Johan de Villiers, Plasma Physics, Nucor, SO AFRICA
Fusion Div. Library, JEN, SPAIN
Prof. Hans Wilhelmson, Chalmers Univ Tech, SWEDEN
Dr. Lennart Stenflo, University of UMEA, SWEDEN
Library, Royal Inst Tech, SWEDEN
Centre de Recherchesen, Ecole Polytech Fed, SWITZERLAND
Dr. V.T. Tolok, Kharkov Phys Tech Ins, USSR
Dr. D.D. Ryutov, Siberian Acad Sci, USSR
Dr. G.A. Eliseev, Kurchatov Institute, USSR
Dr. V.A. Glukhikh, Inst Electro-Physical, USSR
Institute Gen. Physics, USSR
Prof. T.J.M. Boyd, Univ College N Wales, WALES
Dr. K. Schindler, Ruhr Universitat, W. GERMANY
Nuclear Res Estab, Julich Ltd, W. GERMANY
Librarian, Max-Planck Institut, W. GERMANY
Bibliothek, Inst Plasmaforschung, W. GERMANY
Prof. R.K. Janev, Inst Phys, YUGOSLAVIA